# Diffusion enables the distinction between types of tissue microstructure by analyzing the water lineshape

Alexander Ruh[1], Philipp Emerich[1], Dmitry S. Novikov[2], and Valerij G. Kiselev[1]

[1]*Department of Radiology, Medical Physics, University Medical Center Freiburg, Freiburg, Germany,* [2]*Center for Biomedical Imaging, Department of Radiology, NYU School of Medicine, New York, NY, United States*

**Introduction:** Diffusion manifests itself directly in dedicated measurements and indirectly as the driving force behind transverse relaxation in biological tissues. It has been long appreciated that the transverse relaxation is sensitive to the amount of heterogeneously distributed paramagnetic contrast. However, the effects of *spatial arrangement* of tissue susceptibility on $T_2$ measurements remain largely unexplored. Indeed, compartment-exchange models do not explicitly account for susceptibility distribution in real space; the dephasing in the case of slow diffusion is "local", not sensitive to the global distribution properties.

In this work we show analytically and numerically, that weak dephasing in the diffusion-narrowing regime distinguishes between global types of structural organization of tissue susceptibility. As the diffusing spins are probing tissue structure, their relative phases become sensitive to long-range correlations between susceptibility inclusions. Specifically, here we contrast transverse relaxation in a *regular lattice* of permeable spherical susceptibility inclusions (Fig. A1), with that in a *shuffled lattice* (spheres randomly displaced from their lattice positions, Fig. A2), in a packing approximating a *maximally random jammed (MRJ) state* (Fig. A3) [1,2], and in a *disordered packing* with short-range (*Poissonian*) correlations (Fig. A4).

Remarkably, the non-Lorentzian lineshapes for these four media are qualitatively different, so much as to distinguish not only "order" (Fig. A1) from "disorder" (Figs. A2-A4), but also between different *classes* of disorder, which may look very similar to a naked eye (e.g. Figs. A3 and A4). Technically, the difference occurs in the power-law exponent $p$ of the low frequency relaxation "rate" $-\Sigma(\omega)$, ref. [3] and Eqs. (1-3). As the global structural organization is insensitive to local changes, our classification is robust with respect to biological variability between subjects/tissues of similar origin.

Fig. A1: Ordered

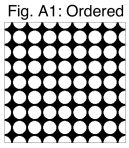

Fig. A2: Shuffled

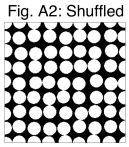

Fig. A3: MRJ

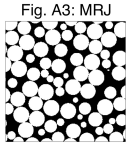

Fig. A4: Poissonian

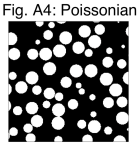

**Background:** To analyze the signal $s(t)$ from a macroscopic sample with a varying Larmor frequency $\Omega(\mathbf{r})$, we utilize the recently developed effective medium approach [3,4], which treats the medium statistically, via the correlation functions of the structural parameters. The resulting spectral lineshape $s(\omega)$ has the universal form given in Eq. (1), where $\Sigma(\omega)$ is the self-energy part [3,4].

$$s(\omega) = \int_0^\infty \mathrm{d}t\; s(t)\, e^{i\omega t} = \frac{1}{-i\,\omega - \Sigma(\omega)} \qquad (1) \qquad\qquad \Sigma(\omega) \approx -\int \frac{\mathrm{d}^3\mathbf{k}}{(2\pi)^3}\, \frac{\overline{\Gamma}_2(k)}{-i\,\omega + D\,k^2}\,, \quad \overline{\Gamma}_2(k) = \langle \Omega_{\mathbf{k}}\Omega_{-\mathbf{k}}\rangle_{\hat{\mathbf{k}}}\,/\,V \qquad (2)$$

When the Larmor frequency variance $\delta\Omega^2 \equiv \langle\Omega^2\rangle$ is small, we can use perturbation theory. In the second order in $\Omega(\mathbf{r})$, the self-energy part is given by Eq. (2), where $V$ is the voxel volume [3]. Here $\overline{\Gamma}_2(k)$ is the angular-averaged Fourier transform of the two-point Larmor frequency correlator $\Gamma(\mathbf{r}) = \langle\Omega(\mathbf{r})\Omega(0)\rangle$. This correlator is proportional to that of the local susceptibility profile, which embodies the microarchitecture [3]. The long-distance behavior of $\Gamma_2(\mathbf{r})$, reflected in the low-$k$ behavior of $\overline{\Gamma}_2(k)$, is crucial to distinguish between different order/disorder classes. Figures B1 and B2 show $\overline{\Gamma}_2(k)$ and the corresponding $\Sigma(\omega)$ [Monte Carlo simulation and numerical calculation using Eq. (2)] for a disordered packing (Fig. A4), ref. [5].

Figure B1

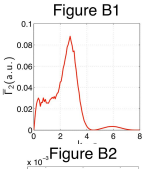

Figure B2

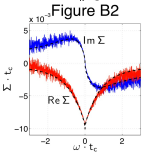


**Simulations**: We generated three-dimensional media made of non-overlapping permeable spheres with radius ρ and constant susceptibility χ. For the disordered medium (Fig. A4), the spheres were randomly added with no overlap, up to a final volume fraction of 35%. For the MRJ medium (Fig. A3), an event-driven molecular dynamics simulation [6] was used to achieve a volume fraction of 65%. To create the shuffled lattice (Fig. A2), the elements of a regular lattice were independently randomly displaced. For comparison we considered an ordered medium (Fig. A1) represented by a simple cubic lattice of spheres. The NMR signal was obtained from Monte Carlo simulations of $10^8$ spins randomly diffusing on a much finer cubic lattice ($1024^3$ sites) with the dephasing strength $\alpha = \delta\Omega\cdot t_c = 0.10$, where $t_c$ is the correlation time to diffuse across the Larmor frequency correlation length, cf. refs. [3,5], which is roughly the sphere size (a natural length scale in the problem).

**Results:** The correlators $\overline{\Gamma}_2(k)$ for small $k$ are depicted in Fig. C for the four media: Disordered (red); MRJ (green); shuffled lattice (black); regular lattice (blue). The correlator $\overline{\Gamma}_2(k)$ for the disordered case has a finite plateau $\overline{\Gamma}_2(+0)$, whereas for the periodic lattice, $\overline{\Gamma}_2(k) \equiv 0$ for small $k$. For the MRJ case, $\overline{\Gamma}_2(k) \sim k$, cf. ref. [2], while for the shuffled lattice, $\overline{\Gamma}_2(k) \sim k^2$. Our main result is that the distinct small-$k$ asymptotes of $\overline{\Gamma}_2(k)$ translate into the distinct small-$\omega$ power law exponents $p$ in $\Sigma(\omega)$:

$$\Sigma(\omega) = \Sigma(0) + \mathrm{const}\cdot\omega^p + \ldots\,, \quad \omega \to 0 \qquad (3)\,.$$

Equation (2) yields $p = 1/2$ for the disordered medium, $p = 1$ for the MRJ state, $p = 3/2$ for the shuffled, and $p = 2$ for the periodic lattice. These exact power laws (dashed lines in Fig. E) agree with the results of numerical integration of the full correlator $\overline{\Gamma}_2(k)$ in Eq. (2) (thick lines in Figs. D, E). We conclude that for small $\omega$, the dominant contribution to $\Sigma(\omega)$ and, thereby, to the lineshape, originates from the small-$k$ behavior of $\overline{\Gamma}_2(k)$.

Our treatment is further verified through the good agreement with MC simulations (noisy lines in Figs. D, E). A minor discrepancy at small $\omega$ (Fig. D) is due to corrections to Eq. (2) from terms higher-order in $\delta\Omega$. We take them into account in a self-consistent way, by shifting $-i\omega \to -i\omega + R_2$ in the denominator of Eq. (2) by the rate $R_2 = -\Sigma(0)$, which is obtained from Eq. (2) for $\omega = 0$. The power law singularity is cut-off for $|\omega| < R_2$, which yields a better agreement (thinner lines in Fig. D), especially for the shuffled and the periodic lattices (blue and black curves).

**Conclusions:** We showed that the NMR spectral lineshape can distinguish between different kinds of global structural organization (order and disorder) of tissue susceptibility. This distinction involves long-range correlations and is thereby robust with respect to the biological variability. The biophysical mechanism behind this phenomenon is the molecular diffusion mediating the spin dephasing reflected in the transverse relaxation. Our results provide a framework for novel types of contrast, such as revealing the cellular organization in tissue doped with interstitium-confined contrast agent.

Figure C

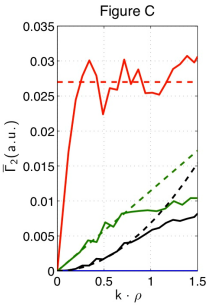


Figure D

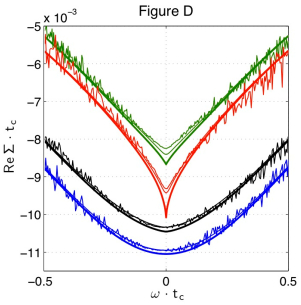


Figure E

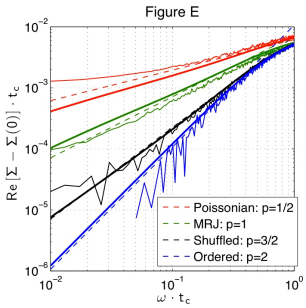


[1] S. Torquato *et al*. Phys Rev Lett 84 (2000) 2064; [2] A. Donev *et al*. Phys Rev Lett 95 (2005) 090604; [3] D.S. Novikov, V.G. Kiselev. J Magn Reson 195 (2008) 33; [4] D.S. Novikov, V.G. Kiselev. NMR Biomed 23 (2010) 682; [5] A. Ruh *et al*. Proc. ISMRM 19 (2011) 1987; [6] M. Skoge *et al*. Phys Rev E 74 (2006) 041127.